Elastic and superelastic properties of $Co_{49}Ni_{22}Ga_{29}$ single crystal

V. A. Chernenko[a),b)]
Institute of Magnetism, Kyiv 03142, Ukraine

S. Besseghini, E. Villa, and A. Gambardella
CNR-IENI, Lecco 23900, Italy

J. I. Pérez-Landazabal
Departamento de Física, Universidad Pública de Navarra, 31006 Pamplona, Spain

(Received 10 March 2007; accepted 21 April 2007; published online 18 May 2007)

Low-frequency-elastic modulus, internal friction, tensile stress-strain loops, and thermally induced strain recovery are studied in the vicinity of the martensitic transformation (MT) exhibited by the [001]-oriented $Co_{49}Ni_{22}Ga_{29}$ single crystal in as-grown state. The mechanical and thermomechanical tests are conducted with TA Instruments Q800 dynamic mechanical analyzer. Elastic modulus shows softening during cooling and a deep minimum at MT concurrently with the abrupt increase of internal friction. The stepwise and jerky yield and recovery of the superelastic 7% strain alongside the appearance of the jumplike character of thermally induced MT are obtained after thermomechanical training. Thermodynamic estimations reveal a self-consistency of the results.
 [DOI: 10.1063/1.2740112]

Among the ferromagnetic Heusler alloys exhibiting thermoelastic martensitic transformation (MT), Co–Ni–Ga alloys are considered to be not only promising candidates for the development of materials with a large magnetostrain effect[1–4] but also materials with large superelastic strains[5,6] and an unusually wide temperature range of superelasticity effect.[5,7,8] Unlike prototype Ni–Mn–Ga, Co–Ni–Ga alloys have enhanced ductility in the cubic phase due to the presence of precipitates of secondary phases,[2,5,8] which guarantee large superelastic strains in various stress conditions including bending and torsion in the case of single crystals doped by Fe atoms.[6]

Whereas previous work with as-grown Co–Ni–Ga single crystals of optimized composition Co(49–50 at. %), Ni(20–22 at. %), and Ga(28–30 at. %) was concentrated on the superelasticity effect under compressive loads,[5–9] the present report extends the study to the temperature dependencies of superelastic loops as measured in tension tests by using a special algorithm implemented in the TA Instruments Q800 dynamic mechanical analyzer (DMA). The abnormally wide temperature range of superelasticity experimentally demonstrated by the present work can be fully explained within the framework of the Clausius-Clapeyron relationship. The additional information derived from the analysis of the elastic and thermoelastic properties, as measured in the tests, also helps fill a gap in the available literature data.

A $Co_{49}Ni_{22}Ga_{29}$ single crystalline ingot with a mass of 80 g was grown by the Bridgman method. One part of this ingot was used previously to study the stress-strain behavior under compressive loading.[5,9] As a result, a superelasticity of 4% and another phenomenon known as the strain-induced stabilization of martensite were found. For the present work, [100]-oriented tensile samples measuring 0.2×0.5 mm^2 in cross section and 6.5 mm as a gauge length, as well as irregularly shaped chips for the calorimetric measurements were prepared from the same ingot. The tensile samples were electropolished to remove the deformed surface layer. The MT temperatures T_M and T_A and the values of latent heat q were determined from the calorimetric curves (Seiko DSC220, 10 °C/min). The aforementioned DMA made it possible to register from the same sample the temperature dependencies of elastic storage modulus $E(T)$ and internal friction (IF), $\tan\delta(T)$, in the dynamic tensile mode, as well as stress versus strain, σ-ε, at a constant temperature T_{exp} and strain versus temperature, $\varepsilon(T)$, at zero stress in the static tensile mode.

The modulus and IF measurements were carried out in the tensile dynamic mode at a frequency of 1 Hz and oscillation strain amplitude of 10^{-4}. The temperature change rate was 2 °C/min. Further details of the dynamic method can be found elsewhere.[10]

After the dynamic measurements, the sample was exposed to a few σ-ε cycles at room temperature using a static tensile mode option of the DMA. Then the mesurements were conducted automatically in the following repeating sequence: (i) annealing at $T_{an}=300$ °C for 10 min and then cooling to the required temperature of the mechanical experiment T_{expt}; (ii) recording of the σ-ε curve at fixed T_{expt}; and (iii) measuring of the heating run $\varepsilon(T)$ in the range from T_{expt} to T_{an}. In the subsequent experiments, the value of T_{expt} was varied step by step from 230 to 70 °C. In these measurements, the upper limit of load, the temperature change rate during heating ramps, and the stress change rate in the mechanical tests were 18 N, 5 °C/min, and 2.5 MPa/min, respectively. The value of annealing temperature and the described sequence of measurement steps were selected to avoid any possible irregularities related to the fact that the specimen superelastic behavior can be very sensitive to the thermal history.

According to our previous structural studies,[5] the thermally induced martensitic phase in the single crystal under study has a $L1_0$ structure with lattice parameters $a_{L1_0}=0.38$ nm, $c_{L1_0}=0.27$ nm, or nonmodulated body centered tetragonal cell with the parameters shown in Table I and $c/a=1.18$. The $B2$ atomic order and value of the cubic

a)Electronic mail: v.chernenko@ieni.cnr.it
b)Present address: CNR-IENI, Lecco 23900, Italy.

TABLE I. MT temperatures T_M and T_A, the transformation heat q, the lattice parameters of the unit cells in pseudocubic coordinate system used for the calculation of transformation strains, and the temperature derivative of the average value of critical tensile stress compared with the calculated one using Clausius-Clapeyron relationship for [001]-oriented $Co_{49}Ni_{22}Ga_{29}$ single crystal.

			Lattice parameters (nm)		Transformation strains				
T_M (°C)	T_A (°C)	q (J/g)	Martensite	$B2$ austenite	ε_{xx}^{tr}	ε_{yy}^{tr}	ε_{zz}^{tr}	$(d\sigma_c^{[100]}/dT)_{expt}^{av}$ (MPa/°C)	$(d\sigma_c^{[100]}/dT)_{calc}$ (MPa/°C)
50	81	2.1	$a_{bct}=0.27$ $c_{bct}=0.32$	$a_c=0.286$	−0.056	−0.056	0.12	0.33	0.41

lattice parameter $a_c=0.286$ nm were identified in the austenitic phase.[5] Also, a small percentage of the fcc γ-phase precipitates was found in the alloy.

The differential scanning calorimetry (DSC) curves and the temperature dependencies of elastic modulus and internal friction for alloy under study are presented in Fig. 1. These dependencies show only one reversible MT taking place in the studied temperature range. The characteristics of MT are given in Table I.

Figure 1 provides the experimental evidence of an anomalous low value of modulus in a wide temperature range and a modulus softening preceding MT with a slope equal to 17 MPa/°C. Similar peculiarities were observed in the case of Ni–Mn–Ga.[11] According to Fig. 1, a lattice instability is characterized by a deep minimum of modulus at MT concurrently with jumplike appearance of IF in the martensitic phase. The enhanced level of tan δ is due to an intrinsic contribution of the highly mobile twinning structure of martensite. The results depicted in Fig. 1 and stress-strain behavior at 60 °C shown in Fig. 2 are representative of the nondeformed sample.

In this work we found by checking several samples that once the forward MT was stress induced in the initial austenite, the martensitic phase formed and the related deformation of 6%–7% disappear in an abrupt manner during a following heating, as shown in Fig. 3. As a result of such a thermomechanical training, the subsequent σ-ε dependence becomes multistep and jerky (Fig. 2). By the DSC measurements illustrated in the inset to Fig. 3, we show that while the reverse MT in a first heating after deformation can be observed in the range of 100–220 °C (which is far away from T_A), the subsequent zero-stress heating/cooling runs confirm transformation temperatures determined for the untrained alloy and shown in Table I. The different character of MT before and after the training can be appreciated by comparison of the DSC curves: a broad nonsymmetric maximum in Fig. 1 is split into several sharp peaks, as seen in the inset to Fig. 3.

The jerky character of MT in the σ-ε and $\varepsilon(T)$ curves (Figs. 2 and 3) and the abnormally high and random temperatures of the strain recovery in Fig. 3 corroborate a strong martensite stabilization in Co–Ni–Ga alloy[5,9] not typical of the other ferromagnetic shape memory alloys.[5,12] The difficulties in forming a habit plane between austenite and the detwinned martensite were considered to be an origin of the mechanical stabilization effect.[5,13] On the other hand, the step-wise character of MT may be ascribed to the nonuniform distribution of the internal stresses in the sample after the aforementioned thermomechanical training. The local elastic fields can be conserved, e.g., near γ-phase precipitates, which basically serve as pinning centers of different strengths capable of hindering the movement of the interfaces. In fact, large energy barriers related to the pinning centers were considered in Refs. 6 and 14 to be the main mechanism leading to the sharp MT. Note that the stress-

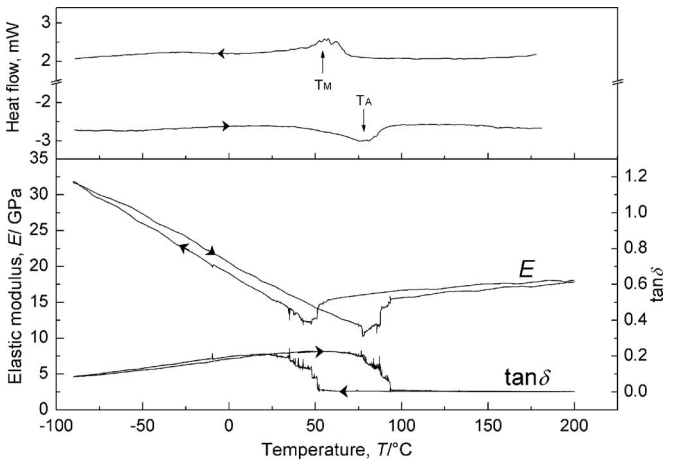

FIG. 1. Heating-cooling DSC thermograms and temperature evolutions of the elastic modulus (E) and internal friction (tan δ) of nondeformed $Co_{49}Ni_{22}Ga_{29}$ single crystal. The martensitic transformation temperatures are shown by arrows.

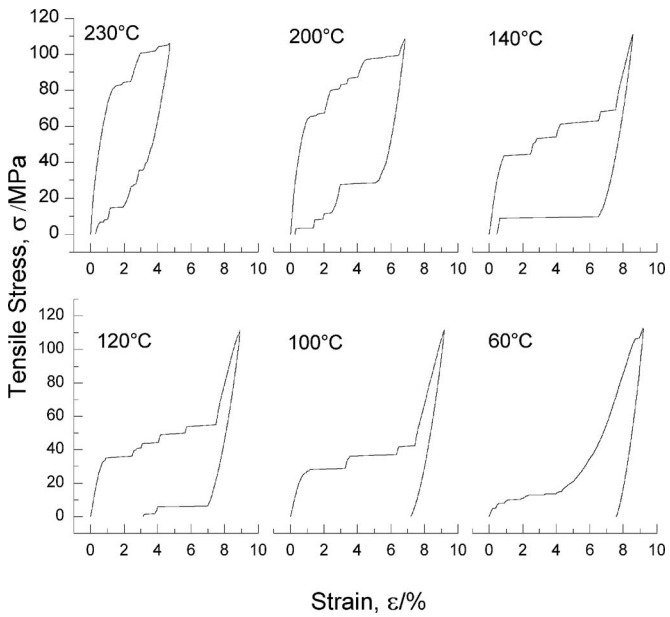

FIG. 2. Selected tensile stress-strain curves from the measurements taken on the [100]-oriented $Co_{49}Ni_{22}Ga_{29}$ single crystal. The measurements are made first at $T_{expt}=60$ °C, then in a sequence from 230 to 70 °C (see text for details).

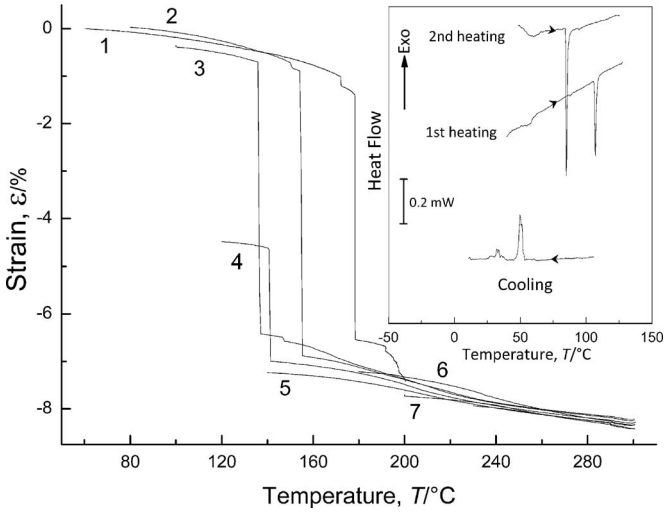

FIG. 3. Selected thermally induced strain recovery (contraction) of the specimen tested in tension (Fig. 2) during heating from T_{expt} to 300 °C. Curves 1–7 correspond to T_{expt}=60, 80, 100, 120, 140, 180, and 200 °C, respectively. The measurements are made first at T_{expt}=60 °C, then in a sequence from 230 to 70 °C (see text for details). Inset: an example of the first heating DSC curve after specimen transformation-induced deformation at 70 °C. The second complete thermal cycle is also shown.

dependent deviation of the habit plane from an invariant plane is an important factor regulating superelastic deformation.[15]

One of the most prominent experimental results obtained in this work is the unusually low temperature derivatives of the critical stresses of the forward (σ_c^f) and reverse (σ_c^r) martensitic transformations: 0.40 and 0.25 MPa/ °C, respectively. These values are obtained as the slopes of the straight lines depicted in Fig. 4. The dependencies in Fig. 4 are the linear approximations of σ_c^f and σ_c^r data points determined by a tangential method from the σ-ε loops (some of them are shown in Fig. 2). The slope of a quasiequilibrium stress-temperature phase diagram given in Table I is obtained by averaging the aforementioned slopes. A substitution of the experimental values from Table I into the generalized Clausius-Clapeyron equation derived in Ref. 16

$$\left(\frac{d\sigma_c^{[100]}}{dT}\right)_{\text{calc}} = \frac{qm}{T_{\text{tr}}\varepsilon_{zz}^{\text{tr}}}, \tag{1}$$

where q, $T_{\text{tr}}=(T_M+T_A)/2$ and $\varepsilon_{zz}^{\text{tr}}$ is the transformation heat, equilibrium temperature of MT and transformation strain component along [100] direction, respectively, yields 0.41 MPa/ °C. This value can be considered as a fairly good approximation to the experimental one whereby a conclusion can be drawn that an unusually wide temperature range of the superelasticity effect is basically explained by thermodynamic considerations.

The monotonous increase of the stress hysteresis with temperature observed in this work (Figs. 2 and 4) is assumed to be rather a result of the temperature-dependent strain-induced stabilization of martensite and associated incompatibility between twinned/detwinned martensite and austenite than dissipation losses related to the possible formation of irreversible lattice defects.[5,12,13,15]

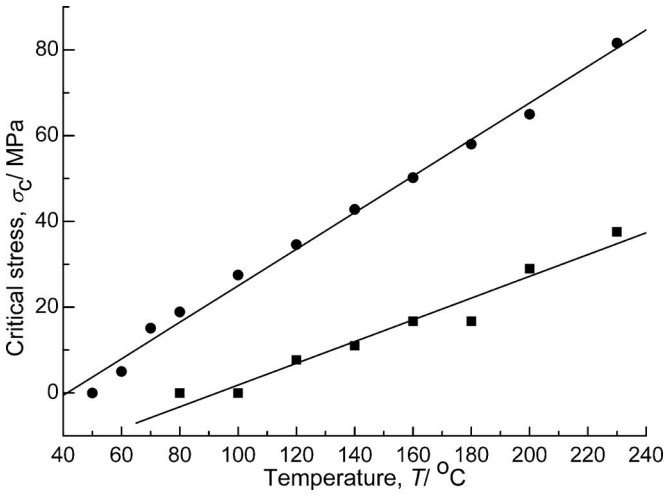

FIG. 4. Tensile stress-temperature phase diagram of [100]-oriented $Co_{49}Ni_{22}Ga_{29}$ single crystal showing the dependencies of the critical stress for the forward, σ_c^f (circles) and reverse, σ_c^r (squares) MT. A linear approximation of the data points is used.

This work was made possible by grant from Fondazione Cariplo (Project No. 2004.1819-A10.9251). The authors thank G. Carcano and S. Pittaccio for technical support. Partial support from the DGI (Ministerio de Ciencia y Tecnologia, Project No. MAT2006-12838) is acknowledged.

[1] M. Wuttig, J. Li, and C. Craciunescu, Scr. Mater. **44**, 2393 (2001).
[2] K. Oikawa, T. Ota, F. Gejima, T. Ohmori, R. Kainuma, and K. Ishida, Mater. Trans. **42**, 2472 (2001).
[3] M. Sato, T. Okazaki, Y. Furuya, and M. Wuttig, Mater. Trans. **44**, 372 (2003).
[4] Y. X. Li, H. Y. Liu, F. B. Meng, L. Q. Yan, G. D. Liu, X. F. Dai, M. Zhang, Z. H. Liu, J. L. Chen, and G. H. Wu, Appl. Phys. Lett. **84**, 3594 (2004).
[5] V. A. Chernenko, J. Pons, E. Cesari, and I. K. Zasimchuk, Scr. Mater. **50**, 225 (2004).
[6] X. F. Dai, G. D. Liu, Z. H. Liu, G. H. Wu, J. L. Chen, F. B. Meng, H. Y. Liu, L. Q. Yan, J. P. Qu, and Y. X. Li, Appl. Phys. Lett. **87**, 112504 (2005).
[7] J. Dadda, H. J. Maier, I. Karaman, H. E. Karaca, and Y. I. Chumlyakov, Scr. Mater. **55**, 663 (2006).
[8] J. Liu, H. Xie, Y. Huo, H. Zheng, and J. Li, J. Alloys Compd. **420**, 145 (2006).
[9] V. A. Chernenko, J. Pons, E. Cesari, and A. E. Perekos, Mater. Sci. Eng., A **378**, 357 (2004).
[10] E. Cesari, V. A. Chernenko, V. V. Kokorin, J. Pons, and C. Segui, Acta Mater. **45**, 999 (1997).
[11] V. A. Chernenko, J. Pons, C. Segui, and E. Cesari, Acta Mater. **50**, 53 (2002).
[12] R. F. Hamilton, H. Sehitoglu, C. Efstathiou, H. J. Maier, and Y. Chumlyakov, Acta Mater. **54**, 587 (2006).
[13] C. Picornell, J. Pons, and E. Cesari, Acta Mater. **49**, 4221 (2001).
[14] X. F. Dai, H. Y. Wang, L. J. Chen, X. F. Duan, J. L. Chen, G. H. Wu, Hao Zhu, and J. Q. Xiao, J. Cryst. Growth **290**, 626 (2006).
[15] A. L. Roytburd, Mater. Sci. Forum **327–328**, 389 (2000).
[16] K. Otsuka and C. M. Wayman, in *Shape Memory Materials*, edited by K. Otsuka and C. M. Wayman (Cambridge University Press, Cambridge, 1998), p. 27.